A multi-service approach for planning the optimal mix of energy storage technologies in a fully-renewable power supply

J. Haas[a*], F. Cebulla[b], W. Nowak[a], C. Rahmann[c], R. Palma-Behnke[c]

[a]*Department of Stochastic Simulation and Safety Research for Hydrosystems (IWS/SC SimTech), University of Stuttgart, Germany*
[b]*Department of Systems Analysis and Technology Assessment, Institute of Engineering Thermodynamics, DLR, University of Stuttgart, Germany*
[c]*Energy Center, Department of Electrical Engineering, University of Chile, Chile*

ABSTRACT

Energy storage systems (ESS) are a structural solution for the integration of renewable energy systems. To plan the optimal combination of ESS, storage expansion planning approaches are commonly used. They tend to focus on balancing the energy fluctuations from renewable technologies but are usually blind to the need for specific additional services required for dealing with forecast errors. Hence, they underestimate the real operating costs of the future power system and lead to suboptimal investment recommendations. In response, we propose a multi-service storage expansion approach.

A linear programming optimization is developed, LEELO, to find the optimal investments in a 100% renewable system (based on solar photovoltaic and wind power) deciding on renewable generators and storage systems. In our formulation, we explicitly model the provisioning of power reserves and energy autonomy as additional services. A case study applies our model to Chile considering four regions and the (existing) hydropower park, for a complete year with an hourly resolution. We systematically assess how our novel multi-service planning differs from conventional energy-based planning in terms of total costs, operation, and investment decisions (with a focus on ESS).

Considering power reserves and energy autonomy reveals on average 20% higher costs that otherwise would not be captured in the expansion planning process. Regarding operation, ESS show only slight differences in the two planning models. All ESS participate in the provision of energy. As might be expected, batteries are the main provider of (short-term) power reserves, assisted by pumped-hydro, whereas hydrogen storage is responsible for providing (long-term) energy autonomy. However, the storage investment decisions differ significantly between both models. In our multi-service model, the attained power capacities and energy capacities are up to 1.6 and 3.2 times larger, respectively than in conventional planning. The resulting storage mix changes even more strongly: a general shift towards hydrogen systems is observed. Mainly batteries are substituted, while pumped-hydro capacities stay relatively constant. The trend of the above results is consistent for various scenarios of wind and photovoltaic generation and for sensitivities of service parameters.

Our findings underline the importance of modeling multi-services in the planning of renewable-based power systems.

Keywords: generation expansion planning; flexibility; integration of renewable technologies; low-carbon systems; electrical energy storage; Paris Agreement;

1 Introduction

For a sustainable development of our society, energy production needs to turn away from fossil sources. More precisely, to meet the goal of the Paris Agreement of keeping the world's temperature increase well below 2 °C, the greenhouse gas emissions need to become *net* zero (for all energy sectors) shortly after the year 2050 [1]. Many countries are already increasingly deploying renewable technologies. However, for reaching 100%-renewable energy systems, higher levels of flexibility are still needed to affront their temporal and spatial variability and uncertainty. In the power sector, flexibility can be provided by the demand side (smart consumers, demand-side management) [2], the supply side (flexible generation, including curtailment of renewable technologies) [3], and infrastructure of transmission and storage [4]. Interconnecting the different energy sectors (power, transport, heat) is another alternative to upgrading the flexibility levels [5].

Energy storage systems (ESS) are widely envisioned as a structural solution for attaining highly renewable systems. Beyond the use of traditional pumped-hydro storage (currently about 170 GW / 1600 GWh worldwide [6]), the deployment of battery energy systems is rapidly growing [6]. Li-ion batteries show an especially promising future due to their fast cost decrease in recent years [7]. Currently, there is more than 2 GW / 6 GWh of installed power/energy capacity worldwide, with much more on the way [6]. To buffer very short-term power fluctuations, flywheels have been widely used to improve system stability, comprising about 1 GW of installed power capacity with a couple of minutes of energy storage [6]. For seasonal storage, hydrogen systems are an option that is receiving substantial research efforts [8]. After the production of hydrogen, it can be stored as such and then be used in fuel cells (for converting it back to power). Alternatively, it can be transformed into methane to be stored in the existing gas infrastructure. From there it can follow the conventional uses of natural gas, such as being burnt in gas turbines. This sector coupling capability is what makes hydrogen so promising, although its currently installed capacity is rather small (<0.1 GW / <0.1 GWh) [6]. Compressed air energy systems can also serve the long-term [9]. However, beyond the two older installations, McIntosh and Huntdorf (from 1978 and 1991), which add up to 0.4 GW / 5 GWh, no further significant installations have been concreted [6].

There are many studies available that size the general storage need in renewable systems. Reference [10], for example, compares almost 20 publications about the ESS requirements in the U.S. and Europe for increasing shares of renewables. Many of these publications do not account for the different storage technologies, although they strongly differ from each other. Batteries, for example, show low costs per power capacity but high costs per energy capacity. The opposite is true in long-term storage technologies, such as hydrogen systems. As no single ESS outperforms all others, the resulting question is what *combination* of storage technologies can offer the least-cost and most reliable solution for future power systems. Thus, more recent studies have included multiple storage devices into their planning programs in the last couple of years. For example, reference [11] focuses on the short-, mid-, and long-term storage needs of Europe. Reference [12] also searches for the storage mix but considers the Middle East and Northern Africa (in addition to Europe). The team of Breyer has assessed the storage requirements for several regions, including Ukraine [7], Turkey [13], and Australia [14]. Many more approaches of storage planning can be found in the literature; reference [15] systemized about 100 publications, including the current challenges.

Three main challenges need to be tackled when planning storage systems for high shares of renewable technologies: variability (in time), site-specificity (or variability in space), and uncertainty (or forecast errors) of renewable generation [15]. The first challenge is frequently addressed by using a sequential time treatment. In generation planning this used to be representative weeks, but current storage planning models tend to plan full years with hourly resolution (i.e. 8760 continuous time steps) [15]. The second challenge can be handled by considering multiple sites for potential projects (where care has to be put on the correlation of the resources), which also implies that the transmission infrastructure has to be modeled (i.e. losses and bottlenecks). The third and last challenge can be tackled by using scenario analysis (e.g. assessing the system's reliability in different meteorological years), robust programming (i.e. finding designs that work for many different conditions —which are already taken into account during the investment planning—), and stochastic optimization.

Stochastic optimization treats uncertainties endogenously by using probabilistic descriptions of the random processes. In other words, the profiles of renewable production are generated within the optimization under the assumption of imperfect foresight [16]. Although this is the most complete approach to handle uncertainties, it is also intensive in computing times; thus, stochastic optimization is mainly found when planning smaller systems, such as distribution grids. Here, the literature shows to be more advanced. Reference [17], for example, introduces an explicit stochastic formulation to deal with forecast errors of load and wind, when sizing distribution system components (like substations or feeders). Reference [18] puts more emphasis on the sources of uncertainty, extending them to emission prices and demand growth. Finally, also with explicit consideration of stochasticity, storage systems and demand response [19], and capacitor banks [20] have been sized. However, when it comes to sizing larger power systems, explicit stochastic approaches are (still) uncommon. In fact, most of the above-cited studies, including the ones analyzed by the reviews in references [21] and [10], either neglect uncertainty, or treat it with scenario analysis.

An emerging alternative to (implicitely) treat uncertainty in large power systems is modeling system services, for example power reserves. Here, the model would request to allocate a buffer among generation and storage units to accommodate for short-term forecast errors (which, in turn, can be described with a statistical parameter, say 10% of the forecasted energy or a percentage). One of the few examples is reference [22], that sized a single storage technology while taking into account power reserves and security requirements. In this line, the most complete work found is reference [23], which presented a detailed formulation of power reserves for planning a thermal-based system (but without considering the transmission system) with

increasing shares of renewables. Modeling such system services can strongly impact the final investment recommendations, and is not fully understood yet.

From the above state of the art, it becomes clear that modeling diverse power system services in planning exercises is a still incipient topic. Consistently, we extend the existing body of literature by understanding how the need for multi-services impacts the optimal combination of storage technologies in a fully-renewable system when including the transmission system. Concretely, this paper contributes by:

i) Assessing how accounting for power reserves and energy autonomy in a storage expansion tool for a multi-nodal system impacts the sizing of multi-storage technologies. We systematically explore these services, focusing not only on the overall costs and investments but also on the crossed-effects among the different storage technologies.

ii) Studying the optimal combination of storage technologies for a projected 100% renewable-based power system that is in line with the Paris Agreement. Beyond wind and solar technologies, the existing hydropower plants (flow routing) are modeled because this technology can alleviate the storage requirements. Including hydropower in such detail and constellation is the first attempt, according to our literature review.

iii) Performing a case study about the Chilean power system. Europe and the U.S. have several studies on fully-renewable power systems, whereas, for South America —and Chile in particular— there are transition scenarios only [10]. In those publications, the focus is typically on the trade-off between conventional technologies and renewables, where storage devices play a minor role only, given the sunk cost of conventional plants. Furthermore, Chile has ambitious renewable targets, including a political goal of reaching 70% of renewable generation by 2050 [24] and research visions of becoming a net solar energy exporter to Latin America [25].

Our findings for a 100% renewable system reveal new and essential long-term insights for planners, modelers, and policy-makers.

The next section details our optimization model used for planning the expansion of energy storage systems considering a multi-service approach. Section 3 presents the description, inputs, and scenarios of the case study (Chile), while Section 4 discusses the results. Finally, Section 5 concludes and lines out the future work.

2 Methods

Our hypothesis is that including power reserves and energy autonomy services in a storage expansion model significantly impacts the final storage investment recommendations. In other words, we seek the optimal mix of ESS that offers a combination of services. We study the impact of modeling these multi-services on: i) the system operation, ii) the total costs, and iii) the investment decisions for each storage technology. The resulting numbers are illustrated for a multi-nodal fully-renewable power system (Chile in the year 2050) that includes an important share of hydropower.

2.1 Introduction to the model

We develop a tool for finding the optimal energy storage mix, called Long-term Energy Expansion Linear Optimization (LEELO). It minimizes the investment and operating costs of a power system, deciding the capacities of storage and renewable technologies. Beyond the classical energy balance, LEELO can include power reserves and energy autonomy as services. Our approach considers a one-year modeling horizon with hourly resolution (i.e. 8760 sequential time steps). The electrical power system is represented by multiple nodes, where the transmission system is modeled as a transport model. Flow routing is modeled to capture cascading hydropower. LEELO can handle any number of storage devices, but in the case study we consider three types: Li-ion battery systems, pumped-hydro systems, and hydrogen systems (more details provided in Section 3.4). We do not model the distribution grid, nor the heat and gas sectors (helpful formulations for those aims are found in references [26] and [27], respectively). As we focus on a 100% renewable-based power system, unit commitment constraints are not necessary (e.g. minimum online/offline times of fossil generators). LEELO is formulated as a linear program in GAMS [28] and can be solved with a barrier (interior point) algorithm, e.g. from CPLEX [29].

We produced two versions of LEELO, one with and one without multiple services:

- Model B (for "basic") is a classical storage expansion problem with energy balance as the main constraint. Relevant inputs are the (projected) load, (projected) costs of deploying and operating storage and renewable technologies, and the primary energy profiles (solar, wind, water) for renewable generation. The model also captures cascading hydropower systems.
- Model M (for "multi-services") extends the previous model by including the following power system services: a) operating power reserves to cope with forecast errors, following grid operator's practices of leaving operational margins as a function of the renewable production. And b) energy autonomy, i.e. leaving energy reserves in storage devices to deal with major, unexpected drops in energy production (e.g. weeks of extremely low renewable generation as when compared to the typical weather year, sometimes referred to as dark doldrums).

In the following subsections, we describe LEELO, starting with the objective function and continuing with the constraints that cover the modeling of the power system, storage technologies, hydropower plants, and renewable technologies. The complete nomenclature including sets, parameters, and decision variables is in the Appendix (Table 8).

2.2 Objective function and decision variables

The objective function is a minimization of investment and operating costs including:

- annualized investment costs of storage in terms of energy capacity and power capacity,
- annualized investment costs of renewable generators,
- variable operating costs of storage for charging and discharging,
- variable operating costs of renewable generators and transmission lines,
- fixed operating costs of storage in terms of installed energy capacity and power capacity,
- fixed operating costs of renewable generators and transmission,
- other costs, such as penalties for unserved energy, curtailed energy, and fictitious inflows.

On the investment side, decisions are related to the power capacity and energy capacity of the storage devices, and the power capacity of the renewable power plants. For the operation, the *main* decision variables are the generated renewable energy, the charged and discharged energy of the storage units, and the transmitted power between the zones. For model M, further operational decision variables include the power system services (see section 2.3.3 and 2.3.4).

2.3 Modeling of power system

2.3.1 Transmission

The transmission system is modeled using a transport model (i.e. only active power flows are considered, and the angle difference of the voltage phasors are not), such as in references [4] or [30]. We assume the losses to be proportional to the transmitted power. This proportion is a combination of a fixed term (transformer) and a variable term (line length). The resulting losses are allocated equally at both ends of the line. The involved equations are not shown here for the sake of brevity. Expansion of transmission is not considered. Although this is a common simplification storage expansion publications [31,32], it might also be a strong one [4]. However, planning transmission infrastructure usually involves other dimensions beyond costs, such as social opposition that results in delays and cost over-runs. These are being dealt with in more detail in an ongoing study.

2.3.2 Nodal energy balance

The energy supplied by renewables r (including hydropower plants h) and storage systems s must match the demand for every time step t at each zone z of the network (Eq. 1). In case of energy shortage or energy surplus, the model gives the option for unserved energy (as this variable is heavily penalized in the objective function, it does not become positive but is useful for tuning purposes) and curtailed energy, respectively. Energy can be exchanged (imports, exports) between nodes.

$$\sum_r p_{r,t,z} + \sum_s (p_{s,t,z}^{charge} - p_{s,t,z}^{discharge}) + p_{z,t}^{unserved} - p_{z,t}^{curtailed} + \sum_{zz} (p_{zz,z,t}^{imp} - p_{z,zz,t}^{exp}) = Load_{t,z}, \qquad \forall t, z \qquad \text{Eq. 1}$$

In traditional expansion planning models, adequacy used to be the other main equation. Essentially, it ensures that the installed generation capacity exceeds the peak demand. However, in systems based on variable renewable generation, the investments are triggered by critical conditions of the net-load (which is highly variable) along the year. In our model, adequacy is, hence, captured in the set of equations represented by Eq. 1.

2.3.3 Power reserves

There are many reserve definitions available in the literature, related to power system security. Here, we distinguish between contingency reserves and operational reserves. The former are needed during contingencies to compensate for the unexpected loss of a generation unit. The latter deal with hourly forecast errors of renewable generation (i.e. steady-state from a power system regulation perspective).

The contingency reserves are equal to the installed capacity of the largest generation unit (Eq. 2). To avoid formulations with integers, we assume that the largest unit is always online. The operational reserves (Eq. 3) are modeled as a percentage of the forecasted renewable energy production. We treat demand as a deterministic process, because its behavior is already well-understood by transmission system operators, and smart systems will only improve the controllability on the demand side. Note that the above ways of sizing the power reserves do not include network allocation's criteria (i.e. independent of the location). Thus, the index b does not appear in the equations.

$$fRes_t^{system} = P^{largest\ unit}, \qquad \forall t \qquad \text{Eq. 2}$$

$$oRes_t^{system} = F^{renewables} \sum_{z,r} P_{r,t,z}^{ins} Profile_{r,t,z}, \qquad \forall t \qquad \text{Eq. 3}$$

In our formulation, storage devices and hydropower reservoirs can endogenously decide what reserves to offer. The sum of reserves offered must always be larger than the reserves requested by the whole power system (Eq. 4 and Eq. 5). The total committed power output of a generator (i.e. the sum of dispatched power, committed operational reserve, committed contingency reserve) has to be smaller than its power capacity. Eq. 6 exemplifies this for a hydropower reservoir. Eq. 7 makes sure that ESS and hydropower offer reserves only if they have enough energy stored to provide them for at least one time step.

In contrast to our linear formulation of reserves, in unit commitment tools they are usually modeled with integer variables (just as it is the case of on/off states of thermal generators). These formulations are relevant when only a few generation units can provide reserves, and their level of flexibility is poor (large minimum offline times, slow reaction times, etc.). In our system, we assume that many distributed storage devices will exist in a 100% renewable power system. For these situations, operational planning literature shows that linear formulations are a good approximation for integer models [33,34], which confirms our choice for a linear formulation for the sake of solving times.

$$\sum_{z,s} oRes_{t,z,s}^{S} + \sum_h oRes_{t,h}^{H} \geq oRes_t^{system}, \qquad \forall t \qquad \text{Eq. 4}$$

$$\sum_{z,s} fRes_{t,z,s}^{S} + \sum_h fRes_{t,h}^{H} \geq fRes_t^{system}, \qquad \forall t \qquad \text{Eq. 5}$$

$$oRes_{t,h}^{H} + fRes_{t,h}^{H} + p_{t,h} \leq P_h^{ins}, \qquad \forall t, h \qquad \text{Eq. 6}$$

$$(oRes_{t,h}^{H} + fRes_{t,h}^{H})\Delta t \leq stored_{t,h}, \qquad \forall t, h \qquad \text{Eq. 7}$$

2.3.4 Energy autonomy

Energy autonomy (or energy reserves) are helpful to cope with (unexpectedly) prolonged periods of low generation. They are analogous to the previously described operational reserves but are expressed in terms of energy instead of power. So, instead of dealing with short-term forecast errors, energy autonomy is a way of dealing with long-term forecast errors or with situations worse than the ones considered in the typical-weather year. In that sense, they relate to term *adequacy* applied to power system planning.

The amount of the energy autonomy requested by the system (e.g. 1 week) is not well established in the power sector yet, as it is currently not a common service in planning. It will need to become more frequent when designing 100% renewable-based systems, especially under the influence of climate change or when merging with other energy sectors. The German fuel sector, for example, imposes an autonomy equal to a three-months demand [35].

The level of autonomy requested by the system is expressed in hours (in which the system has to be able to satisfy demand without generation) and is transformed into units of energy with Eq. 8. The different storage devices and hydropower reservoirs act together to meet this level at all times (Eq. 9). The amount of energy autonomy that each ESS can offer (in MWh) during a period is bounded by its stored energy (Eq. 10) and by its converter, which limits the energy it is able to evacuate during the respective time horizon (Eq. 11). Eq. 10 and Eq. 11 are analogous for hydropower reservoirs but are not shown for the sake of brevity.

$$Autonomy^{system} \leq Load_{average}^{system} AutomyHours^{system} \quad \text{Eq. 8}$$

$$\sum_{s,z} autonomy_{s,z,t} + \sum_{h} autonomy_{h,t} \geq Autonomy^{system}, \qquad \forall t \quad \text{Eq. 9}$$

$$autonomy_{s,z,t} \leq stored_{s,z,t}, \qquad \forall s,z,t \quad \text{Eq. 10}$$

$$autonomy_{s,z,t} \leq P_{s,z}^{ins\ discharge} AutonomyHours^{system}, \qquad \forall s,z,t \quad \text{Eq. 11}$$

2.4 Modeling of storage technologies

2.4.1 Charging and discharging capacity and energy capacity

The power output (discharge capacity) of an ESS is limited by its installed power capacity (e.g. power of the turbines) in Eq. 12. The charging capacity is assumed to be symmetric (i.e. installed charging capacity equals the installed discharging capacity). Similarly, the stored energy is limited by the installed energy capacity (e.g. volume of the reservoir) in Eq. 13. The power capacity and energy capacity are independent decisions (i.e. disjoint) [36].

$$p_{s,z,t}^{discharge} \leq P_{s,z}^{ins\ discharge}, \qquad \forall s,z,t \quad \text{Eq. 12}$$

$$stored_{s,z,t} \leq E_{s,z}^{ins}, \qquad \forall s,z,t \quad \text{Eq. 13}$$

2.4.2 Energy-to-power ratio

To make sure that the resulting storage investments are of reasonable sizes (i.e. that the ratio between the energy and power capacity is economically meaningful), we limit the energy-to-power ratio with Eq. 14. This constraint avoids, for example, batteries with oversized energy capacities, say 24 hours.

$$F_s^{Min\ E2P} P_{s,z}^{ins\ discharge} \leq E_{s,z}^{ins} \leq F_s^{Max\ E2P} P_{s,z}^{ins\ discharge}, \qquad \forall s,z \quad \text{Eq. 14}$$

2.4.3 Cycling and state-of-health

Some storage technologies have to be replaced after a limited amount of cycles, e.g. batteries. Eq. 15 accounts for this issue by constraining the maximum amount of yearly cycles (discharged energy divided by installed energy capacity) of each storage technology. For example, if the battery system has a lifetime of 10 years and 10,000 cycles, then Eq. 15 makes sure that batteries deliver less than 1000 cycles/year. Note that to keep the linearity of the program, the term corresponding to the installed energy capacity actually goes on the right-hand-side.

$$\sum_{t} p_{s,z,t}^{discharge} / E_{s,z}^{ins} \leq Cycles_s^{max} / Lifetime_s, \qquad \forall s,z \quad \text{Eq. 15}$$

Furthermore, state-of-health refers to the decrease of the storage performance due to aging. Examples are lower storage capacities in batteries (degradation) and lower power capacities in turbines (mechanical wear). Our model does not account for this issue, which is a common simplification in static planning [15].

2.4.4 Energy balance, own losses, start and end conditions

The energy balance (Eq. 16, [37]) in the ESS takes into account the energy taken from the grid for charging (decreased by its charging efficiency) and the energy delivered to the grid for discharging (increased by its discharging efficiency). The stored energy is also decreased by self-discharge, calculated as a fraction of the stored energy (Eq. 17, [37]). Another loss occurs when providing power reserves (Eq. 18). This equation ensures two things. First, it tells the model that the storage technologies with higher round-trip efficiencies might be the first ones in providing these reserves. And second, it accounts for the energy lost in that process (e.g. batteries dedicated to providing frequency reserves is a net energy consumer). These storage conversion losses arise from balancing a sub-hourly cycle (or noise) related to forecast errors, which is superposed to the hourly energy commitment. Furthermore, the offered reserves are not always fully deployed, which is captured with a factor that represents the frequency of fully deploying these (offered) reserves.

$$stored_{s,z,t+1} = stored_{s,z,t} + (\eta_{charge} p_{s,z,t}^{charge} - 1/\eta_{dis}\, p_{s,z,t}^{discharge} - loss_{s,z,t}^{storage} - loss_{s,z,t}^{reserves})\, \Delta t, \qquad \forall s,b,t \quad \text{Eq. 16}$$

$$loss_{s,z,t}^{storage} = (F_{s,z}^{losses}/24)\, stored_{s,z,t}, \qquad \forall s,z,t \quad \text{Eq. 17}$$

$$loss_{s,z,t}^{reserves} = \left(oRes_{t,h}^{S} F^{used\ oRes} + fRes_{t,h}^{S} F^{used\ fRes}\right)\left(1 - \eta_{discharge}\eta_{charge}\right), \qquad \forall s,z,t \quad \text{Eq. 18}$$

The start and end conditions of the stored energy are decision variables. Both are set to be equal to avoid the optimization from draining the stored energy towards the end of the time horizon.

2.4.5 Resource potential

The maximum capacity of to-be-installed storage technologies might be limited. For example, pumped-hydro is constrained to available height differences. These bounds (for energy capacity and power capacity) are expressed by Eq. 19 and Eq. 20.

$$P_{s,z}^{ins\ discharge} < P_{s,z}^{potential}, \qquad \forall s, z \qquad \text{Eq. 19}$$

$$E_{s,z}^{ins} < E_{s,z}^{potential}, \qquad \forall s, z \qquad \text{Eq. 20}$$

2.5 Modeling of cascading hydropower

Cascading hydropower systems are more complex than other storage technologies. The following equations are specific to the former and are additional to the storage equations of Section 2.4. Here, we use a unit-sharp representation for hydropower plants. This approach generates more decision variables but is necessary for capturing the cascades. Technically, it also triggers the need of distinguishing hydropower plants from other storage devices in all equations of the model, but for the sake of simplicity, we tried to group hydro reservoirs and other ESS whenever possible.

2.5.1 Water to power yield

The conversion from water to power depends on many factors (e.g. efficiency, head). These are all summarized in the yield k, which we assumed to be constant (Eq. 21). This value is unique to each reservoir.

$$p_{h,t} = k_h q_{h,t}^{turbined}, \qquad \forall\, h, t \qquad \text{Eq. 21}$$

2.5.2 Flow routing

The connectivity of cascading hydropower plants is modeled with connectivity vectors (a simplified formulation of connectivity matrixes), one for the turbined flows and one for the diverted flows. These indicate from where to where the flows (turbined or diverted) go. For instance, if the hydropower plant hh is immediately upstream of plant h, the corresponding entry in the connectivity vector (row hh) would show the identifier of h.

The turbined flows that come from upstream are computed in Eq. 22. The expression for the diverted flow is analogous.

$$q_{h,t}^{turbined\ upstream} = \sum\nolimits_{hh} q_{hh,t}^{turbined}, where\ hh\ are\ immediately\ upstream\ of\ h, \qquad \forall\, h, t \qquad \text{Eq. 22}$$

2.5.3 Water balance

The water balance (Eq. 23) is analogous to the energy balance of the storage devices but involves more terms. The water additions (Eq. 24) contain the natural inflow, the diverted and turbined flows from upstream (as explained above), and the fictitious flows. The latter is a tuning variable with correspondingly high penalties in the objective function. Clearly, in the results of the case study, this variable needs to be zero. The water output (Eq. 25) includes the turbined and diverted flow (by the corresponding hydropower plant), and the flow used for the provision of the power reserves (analogous to Eq. 18).

$$stored_{h,t+1} = stored_{h,t} - loss_{h,t} + \left(q_{h,t}^{in} - q_{h,t}^{out}\right)\Delta t, \qquad \forall\, h, t \qquad \text{Eq. 23}$$

$$q_{h,t}^{in} = Q_{h,t}^{inflow} + q_{h,t}^{diverted\ upstream} + q_{h,t}^{turbined\ upstream} + q_{h,t}^{fictitious}, \qquad \forall\, h, t \qquad \text{Eq. 24}$$

$$q_{h,t}^{out} = q_{h,t}^{turbined} + q_{h,t}^{diverted} + q_{h,t}^{reserve}, \qquad \forall\, h, t \qquad \text{Eq. 25}$$

2.6 Modeling of renewable technologies

2.6.1 Max. power capacity

Wind, solar PV, and run-of-river hydropower are modeled as follows (for cascading hydropower, read above). The generated power is limited by the installed capacity in Eq. 26 (which also is decided by the model). It is further constrained by the available natural resource (wind, sun, water), which has a resolution in time and space (Eq. 27). To reduce computing time, we set the generated power equal to the available energy profile. All energy excesses are handled with the variable for energy curtailment, which is indexed per node (recall Eq. 1) instead of per generator and thus reduces the computational effort.

$$p_{r,t,z} \le P_{r,z}^{ins}, \qquad \forall\, r, t, z \qquad \text{Eq. 26}$$

$$p_{r,t,z} = P_{r,t,z}^{ins} Profile_{r,t,z}, \qquad \forall\, r, t, z \qquad \text{Eq. 27}$$

2.6.2 Curtailment

We limit the maximum amount of curtailed energy since large quantities could render the investment unattractive (Eq. 28). In other words, instead of installing excessive generation that could be curtailed, this equation makes sure that the produced energy is preferably used or stored. Limits extremely close to zero seem to produce biased results towards the energy capacity of storage [10], but values between 5% and 20% have shown to be reasonable in the literature [10]. The curtailed energy is (slightly) penalized in the objective function.

$$\sum\nolimits_{z,t} p_{z,t}^{curtailed} \le P_{max}^{curtailed} \sum\nolimits_{r,t,z} Profile_{r,t,z}\, P_{r,z}^{ins} \qquad \text{Eq. 28}$$

2.6.3 PV-to-wind ratio

Previous studies show that one of the leading drivers of different storage requirements is the power mix [10]. To explore a wide range of possible future power systems, we impose the proportion of the to-be-installed capacities between PV and wind (Eq. 29). The model still decides where to invest but needs to respect this PV-to-wind ratio.

$$\sum_{r=PV,z} P_{r,z}^{ins} = PVtoWindRatio \sum_{r=wind,z} P_{r,z}^{ins}, \qquad \forall z \qquad \text{Eq. 29}$$

2.6.4 Resource potential

The resource potential is expressed in the same way as for storage technologies (Eq. 19). The corresponding inputs are typically taken from existing resource-mapping studies.

3 Case study

This section will describe the inputs of the case study. Following the structure of the previous section, we will first present an overview of the system under study, and then detail main inputs and assumptions for the optimization model. At last, the scenarios considered for the model runs are defined.

3.1 Description of system

We used a brownfield planning approach to design Chile's power system in 2050, deciding the investments of renewable generation and storage technologies. However, the subsequent analysis of results will focus on the storage decisions only. From the current power system, we assumed that only the existing hydropower plants and transmission lines -given their long lifetime- will be present in 2050, while thermal power plants will be fully decommissioned. We modeled Chile in four zones (see Fig. 1 for those zones, including main results). Each zone includes three profiles (or locations) for both wind and solar technologies and two profiles for run-of-river plants. From south to north these zones are:

- Southern Chile (z_1): with large cascading hydropower capacity, outstanding wind sites, but only limited potential for solar technologies. The demand is mainly residential.
- Central Chile (z_2): many cascading hydropower plants, good sites for wind and PV generation. Most of the country's load is concentrated here, presenting a mix of residential and industrial profiles.
- Southern Atacama (z_3): excellent wind and outstanding solar potential. The demand is small and mainly industrial.
- Northern Atacama (z_4): excellent wind and outstanding solar potential. The load is industrial.

3.2 Inputs for the objective function

Here, we describe the main parameters. The complete set of values can be found in online [38].

3.2.1 Costs parameters

The costs and lifetime of the different storage technologies and renewable technologies are taken from reference [7]. This database uses experience curves to project costs to the year 2050 and has been validated in numerous journal publications [13,39]. For pumped-hydro, we used a capital cost for power and energy capacity of 1100€/kW and 10€/kWh, which is consistent with reference [40].

3.2.2 Penalties

The penalty cost for unserved energy is set to 10k€/MWh. Fictitious inflows are punished more strongly to avoid them becoming positive. A cost of 5€/MWh is used for curtailed energy.

3.3 Inputs for the power system

3.3.1 Transmission

The existing power transmission capacities are based on the databases of the power system operator [41]. Each zone is interconnected to the adjacent ones by transmission lines of approximately 1.5–2.0 GW of capacity. We modeled linear losses equal to 1.5% (of the transmitted power) per 1000 km [42].

3.3.2 Load

The yearly load profiles (with hourly resolution) of zones z_1, z_2, and z_3 are based on data of [43], and of zone z_4 on [41]. These are then projected to 2050 using the growth rates given by Chile's National Energy Commission [44][1]. This results in an average demand of 3, 12, 2 and 6 GW (23 GW) for the zones z_1 to z_4 and a total peak load of 29 GW.

3.3.3 Power reserves

The contingency reserves are set equal to the installed capacity of the largest generation unit, which is a hydropower reservoir of 0.7 GW. Our first simulations showed that the results are not sensitive to variations from 0.5–1.0 GW. Therefore, the amount of contingency reserves remains fixed during all simulations.

For the operational reserve, we evaluated four cases ranging from 5% to 20% of the forecasted renewable energy production. The upper bound is close to the current practices of some system operators, whereas the lower bound can be understood as a future setting when the forecasts become more precise (better tools and more knowledge).

3.3.4 Energy autonomy

We explored four scenarios of autonomy, specifically 1, 7, 30, and 90 days. The 1-day scenario aims to account for the worst day (e.g. day with very low wind and PV production), which might not be captured in the time series (typical-year) used in this planning exercise. The other extreme, 90 days, is used in the fuel sector of Germany [35]. A substantial autonomy would avoid an energy crisis similar to Chile's in 2007 when it could no longer import gas from Argentina.

[1] This source projects the loads until 2036. To obtain the demand of 2050, we assumed that the growth rate of 2035 would remain constant.

3.4 Inputs for the storage technologies

We considered the following storage systems: Li-ion battery systems (BESS), pumped-hydro storage (PHS), and hydrogen systems (H_2). For hydropower reservoirs, please see the next section. We included Li-ion because of its rapid growth in deployment, PHS because it is a well-established technology, and H_2 as a promising technology in future multi-energy (power-heat-transport) systems.

The technical potential of BESS is virtually unlimited. In the model, we only limit the energy-to-power ratio between 1 and 6 hours. These values are based on the currently installed BESS that show an average of 2 h and an upper limit of 4 h [6]; allowing some room for growth for this ratio as the technology matures.

Regarding PHS, we assumed that about 5 GW of projects could be realized in those zones with already large deployed hydropower capacities (z_1 and z_2). We assumed 3 GW in the zones of the desert (z_3 and z_4), where the main source of water is the ocean (i.e. PHS installed on the cliffs). This equals about ten projects of the size of the ongoing PHS project in the Atacama Desert [45]. We assumed the same costs for both freshwater and seawater PHS systems. We bounded the energy-to-power ratio between 1 and 20 h. The upper limit avoids larger reservoirs (which may face strong social opposition [46]).

For H_2 storage, we considered a chain of systems composed of an electrolyzer (produces H_2 with electricity), a methanizer (converts H_2 to methane for easy storage), a gas tank, an open cycle gas turbine (for reconverting the methane back to electricity), and a CO_2 scrubber (for capturing the CO_2 from the gas turbine and feeding it to the methanizer). The potential of these technologies is unconstrained.

3.5 Inputs for cascading hydropower

We modeled the existing hydropower park given the long lifetime of the technology and the fact that in Chile water licenses do not expire. We assumed that the installed capacity would not grow beyond the existing park [41] because the hydropower sector in Chile has lately shown major difficulties in deploying new projects. Especially large projects are hampered by environmental concerns and social opposition [46,47].

The modeling of the existing hydropower cascades and their connectivity (flow routing) and inflows is based on references [41,43] and [48], respectively. More information can be found in our previous publications [49,50]. The ecological flow is assumed to be ten percent of the maximum power output for the lowest power plant of each cascade. In total, we captured over 40 hydropower plants, with capacities distributed about equally in zone 1 and 2.

3.6 Inputs for renewable technologies

The power generation mix of our case study consists of 100% renewable technologies. We modeled the expansion of solar PV and wind power. We also considered existing run-of-river (in addition to the previously mentioned hydropower cascades), grouped into an equivalent hydropower plant per zone, attaining 0.1, 0.3, 0.1, and 0.0 GW for z_1 to z_4, respectively. Their profile is based on reference [43]. Geothermal and biomass energy in Chile have shown a negligible increase when compared to PV and wind. Hence, they are not included in this study.

We considered single-axis tracking PV plants and onshore variable-speed wind farms. The profiles are generated with the online tools *Solar and Wind Energy Explorer* [51,52]. Details on these tools can be found in [53]. We used 3 locations for solar and 3 for wind in each zone (thus totalizing 24 profiles in the model). Given the vast extension of Chile, the potential of solar and wind are not constrained by space (an overview of other challenges that the solar sector is facing can be consulted in reference [54]).

We study five scenarios varying the ratio between installed PV and wind plants (but all are 100% renewable). These include solar dominated scenarios (PV++ and PV+ with ratios of 3:1 and 2:1) and wind dominated scenarios (Wind++ and Wind+ with ratios of 1:3 and 1:2). The last scenario is a balanced mix (1:1).

3.7 Summary of scenarios

Altogether, we subjected the following parameters to sensitivities: PV-to-wind ratio, autonomy requirements, and reserve requirements. Table 1, provides an overview of the resulting scenarios. The nomenclature of the first column will be used later on in the discussion.

Our base case consists of a balanced mix. Model B does not consider autonomy and reserves, whereas model M prescribes an autonomy of 7 days and operational reserves equal to 10% of the forecasted renewable generation (contingency reserves are always equal to the largest generation unit).

To systematically explore differences in storage decisions as a function of different generation portfolios, we defined a set of scenarios varying the PV-to-wind ratio. In these scenarios, the service parameters are kept constant (same as in the base case). Here, we compared the results from model B with model M.

The second set of scenarios explored different parameters for the services in a balanced mix. Here, we compared the resulting differences from the scenarios with the base case of model M (and not with model B).

Table 1: *Definition of scenarios*

	ID	Model	PV-Wind ratio	Autonomy (days)	Reserve[a]
	Base Case (B)	B	1:1	-	-
	Base Case (M)	M	1:1	7	10%
Sensitivities of power mix	PV+ (B)	B	2:1	-	-
	PV+ (M)	M	2:1	7	10%
	PV++ (B)	B	3:1	-	-
	PV++ (M)	M	3:1	7	10%
	Wind+ (B)	B	1:2	-	-
	Wind+ (M)	M	1:2	7	10%
	Wind++ (B)	B	1:3	-	-
	Wind++ (M)	M	1:3	7	10%
Sensitivities of service	Autonomy 1-day (M)	M	1:1	1	10%
	Autonomy 1-month (M)	M	1:1	30	10%
	Autonomy 1-quarter (M)	M	1:1	90	10%
	Reserve 5% (M)	M	1:1	7	5%
	Reserve 15% (M)	M	1:1	7	15%
	Reserve 20% (M)	M	1:1	7	20%

[a]Percentage of forecasted renewable generation; additionally, we considered a frequency reserve equal to the largest unit.

4 Results and discussion

In this section, after a brief overview of the system, we will analyze the impact of modeling multi-services in storage expansion planning. First, the operation of the storage devices between the two models is contrasted. Then, their cost difference is analyzed and, finally, the effect of modeling multi-services on the storage investment decisions is studied.

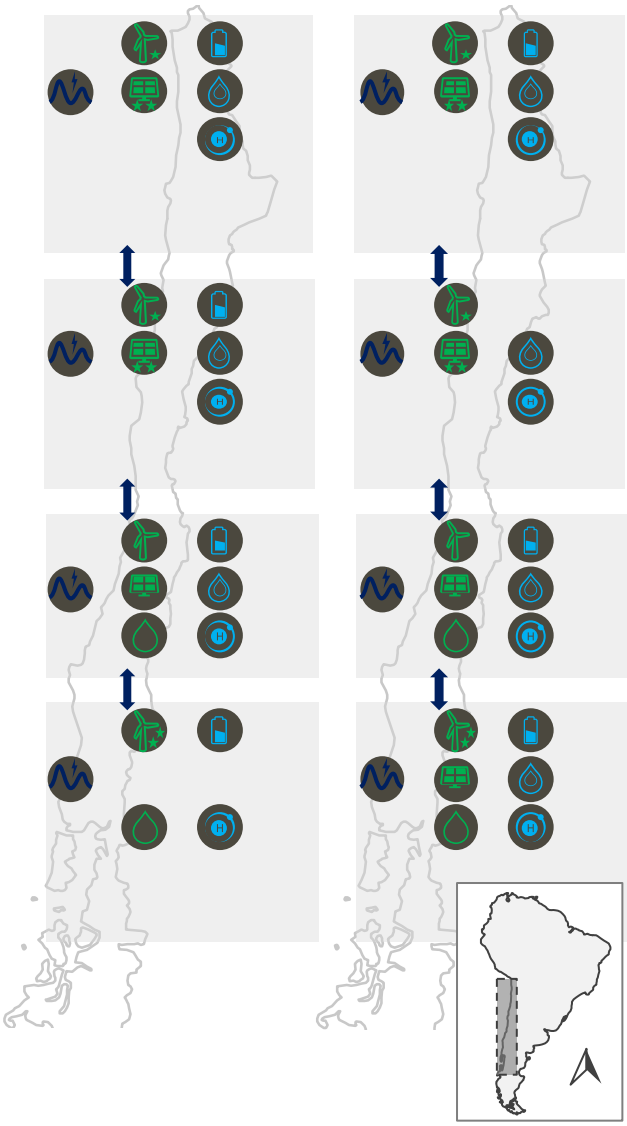

Fig. 1. *Main investment decisions for the Chilean power system in 2050 along the four regions for the scenarios (a) base case and (b) PV++ of model M. Green icons show the generators (solar PV, wind, and existing hydro; zones marked with one/two stars indicates that the resource is excellent/outstanding), light-blue the storage systems (BESS, PHS, and H_2), and dark-blue the load. Numbers show the installed power capacities in GW (and in brackets the storage capacity in full load hours (h) / months (m)).*

Before starting with in-depth analysis, we will first show the main investments to get a general impression of the system. Fig. 1 shows, per zone, the installed capacities of the generation technologies (including existing hydropower cascades), the existing transmission infrastructure, and the planned storage mix. Panel a) shows the base case and panel b) the PV++ scenario, (which we decided to show because it is the most cost-effective one).

In the base case, zone 1 only installs wind turbines supported mainly by the hydropower park and H_2. Zone 2 has more PV than wind generation and requires vast storage facilities of all kinds to supply the main load center. Zone 3 is based more on wind than PV power and needs mainly H_2 assissted by smaller PHS and BESS for balancing renewable generation. Zone 4, is dominated by PV and requires important shares of all storage technologies. H_2 is present in all zones with an energy capacity of around one month, whereas PHS and BESS show capacities of 12-20 h and 2-5 h, respectively.

The PV++ scenario, per definition, relies on solar generation, which compared to the base case creates differences in terms of the storage requirements. Zone 1 decreases the amount of needed H_2 power capacity, which is offset in zone 2. Zone 3 now relies more strongly on PHS. In zone 4, H_2 and PHS remain constant, but batteries double to deal with the fluctuations of a *solar*

pole. Along the four zones, the energy capacities suffer only small changes regarding the base case. In all scenarios, the model does not recommend run-of-river hydropower plants under the used cost assumptions.

This kind of analysis could be deepened, following references [11] or [12], for example. However, now we will focus on the novelty of the present work, which is understanding how accounting for multi-services offered by multi-storages in a multi-nodal system impacts the expansion decisions.

4.1 Operation of storage technologies

Here, we will compare the operational results of model B with model M, to identify what service is provided by each kind of ESS. Fig. 2 summarizes the operation of the different ESS in the base case (of model B and M). Each row corresponds to one storage technology (all storage devices of a same technology –along the four zones– are now grouped). All values are normalized by the installed capacity of each storage technology.

Panel a) and Panel b) of Fig. 2 compare the energy delivery and the state of charge, respectively. These panels show how in both models B and M, BESS and PHS respond to the day-night cycle of solar generation. BESS also follows the variability of wind, presenting an overall more fluctuating behavior. Whereas BESS is fully depleted during the nights, PHS tends to be steadier. H_2 has a more seasonal operation showing high states of charge during summer and low ones during winter. It charges during longer periods (full days or weeks) of solar availability and discharges during shorter times of low energy availability. It contributes to some extent to balancing the day-night cycles. H_2 follows a similar operational pattern as in both models, but consistently operates below its installed capacity in model M. In other words, model M recommends more H_2 converters (triggered by the autonomy criterion) without fully using them. Furthermore, in model M, H_2 is never completely empty (for the same reason).

Panel c) of Fig. 2 shows the provision of power reserve and energy autonomy in the left and right column, respectively (both for model M only). It becomes clear that BESS is the main technology in providing power reserves, assisted by PHS before sunrise (moments of low state of charge). Energy autonomy is steadily provided by H_2 throughout the year and by PHS during the day (except the early morning). BESS seems to help after noon (once they reach a higher state of charge).

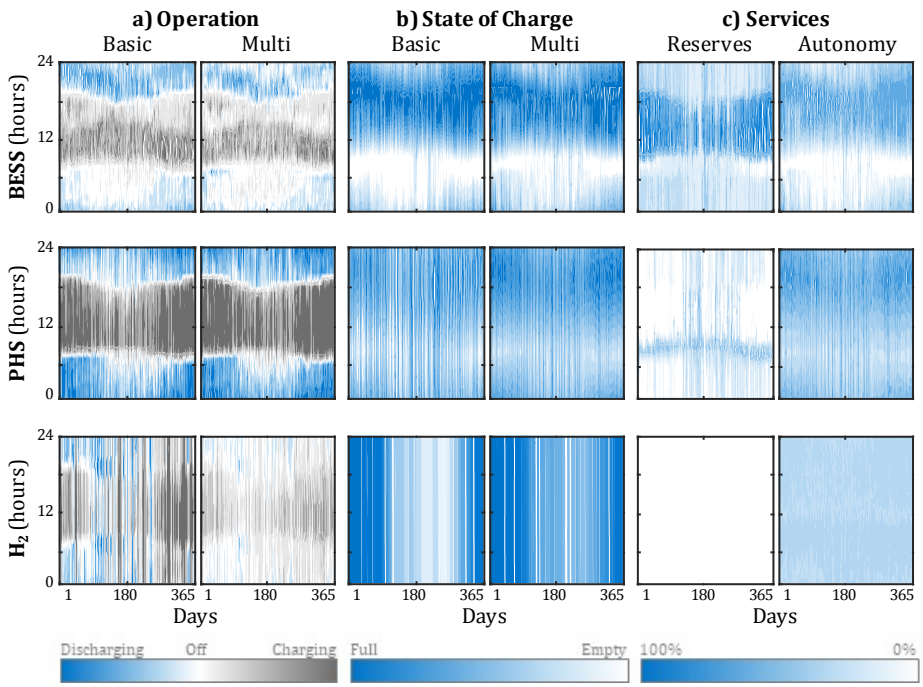

Fig. 2. *Operation of ESS (BESS, PHS, H_2). a) Power output, left: model B, right: M. b) State of charge, left: model B, right: model M. c) Services, left: power reserves in model M, right: energy autonomy in model M. Numbers are relative to the capacity (energy or power) of each ESS.*

Up to this point, we have shown the operation of each storage technology, normalized to its respective installed capacity. Fig. 3 instead normalizes to the total service requested by the power system. It shows one dimensionless index for the provision of energy[2], power reserves[3], and autonomy[4], in the subplots a), b), and c), respectively. Figure 3 clearly illustrates that more than half of the energy is delivered by PHS; followed by BESS and H_2. BESS, despite its small energy capacity (Fig. 4), is still able to provide vast quantities of energy given by the large number of cycles. Power reserves (contingency plus operational) are primarily provided by BESS and PHS. Energy autonomy is virtually only delivered by H_2. This stands in apparent conflict with Fig. 2; although the provision of autonomy by BESS and PHS can be measured when relative to their installed capacities, the absolute magnitude is not relevant from a system perspective.

As a general remark, the intuition that H_2 should focus on energy delivery and that only BESS will provide power reserves does not show to be true. All ESS participate with important shares in delivering energy. Power reserves are met by BESS and PHS. H_2 is the main technology for energy autonomy. When subjecting the parameters of these services to sensitivities, the found operational trends remain consistent (not shown for the sake of brevity).

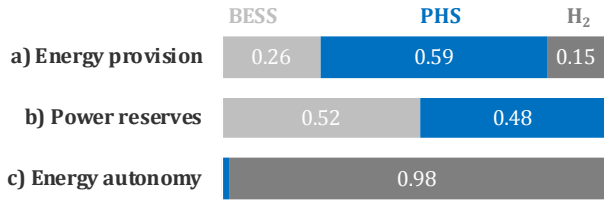

Fig. 3. *Service provision by the different storage technologies. Numbers are relative to the total service requested by the power system.*

4.2 Impact of multi-services on the system costs

In this section, we will look at the cost difference between both models and how these differences are consistent across scenario variations. By definition, model M must show costs greater than (or equal to) model B, because it has more constraints. This difference, however, has to be understood as the error or cost-underestimation of model B. In other words, model M shows a cost closer to reality, which is simply not captured by model B. Table 2 summarizes the total costs obtained by model B and M, divided by the total energy demand (€/MWh).

The impact of planning with multi-services translates into over 20% of total costs difference. This magnitude is consistent for different power mixes (different ratios between PV and wind power), ranging from 16–22%. The smallest difference occurs for mixes based on wind power. Balanced and PV-dominant scenarios are on the other extreme.

Table 2: *Total costs for different scenarios of PV-to-wind ratios, for model B and M*

Case	Cost B (€/MWh)	Cost M (€/MWh)	Ratio M/B (-)
Balanced mix	36.5	44.4	1.22
PV+	35.8	43.8	1.22
PV++	36.2	44.0	1.22
Wind+	39.3	46.6	1.19
Wind++	41.7	48.3	1.16

When analyzing the sensitivity of different service parameters, the cost difference seems (shown in the last column of Table 3) minor. Energy autonomies smaller and larger than one week (base case) impact the costs by -4% and +3%, respectively. Different power reserve parameters have a cost difference below 1%. Hence, the parameters used in the base case (BC) seem robust because further parameter variations produce only slight (additional) cost differences.

[2] Energy provided by one ESS divided by the total energy supplied by all ESS.

[3] Ratio of provided reserves by one ESS and the system-wide requested power reserves (frequency and operational reserves are grouped).

[4] Ratio of autonomy provided by one ESS and the total autonomy offered by all ESS.

Table 3: *Total costs for different parameters of power reserves and energy autonomy, for model M*

Case	Cost M (€/MWh)	% (rel. to BC)
Autonomy 1-day	42.8	0.96
Autonomy 1-week (BC)	44.4	1.00
Autonomy 1-month	44.8	1.01
Autonomy 1-quarter	45.6	1.03
Reserve 5%	44.3	1.00
Reserve 10% (BC)	44.4	1.00
Reserve 15%	44.5	1.00
Reserve 20%	44.7	1.01

In short, considering energy autonomy and power reserves in expansion planning reveals costs that in traditional planning would remain hidden. These costs are on average 20% and are robust for different parameters of these services.

As a general remark, the (mis-) planned power system by model B would need further adaptions or else it may suffer from a poorer quality of service, e.g. unserved energy. This, in turn, implies costs greater than (or equal to) those of model M. In the literature, this is typically assessed by Monte Carlo approaches that test many operating conditions for the recommended investments [55,56]. In our work, however, we did not study the cost over-runs of model B, to focus on the impact on the investment decisions, which we will see now.

4.3 Impact of modeling multi-services on the investment decisions

4.3.1 Base case

We will now analyze the investment decisions when modeling multi-services. For this purpose, Fig. 4 shows the resulting storage investment decisions of the different storage devices for all scenarios (energy capacities in panel (a) —note that the axis is discontinuous for H_2— and power capacities in panel (b)). For example, in the base case, model B suggests a total storage requirement of 3.4 TWh and 20.7 GW, while model M recommends 10.7 TWh and 32.1 GW. This is an increase by a factor of about 3.2 and 1.6 for the energy and power capacity, respectively.

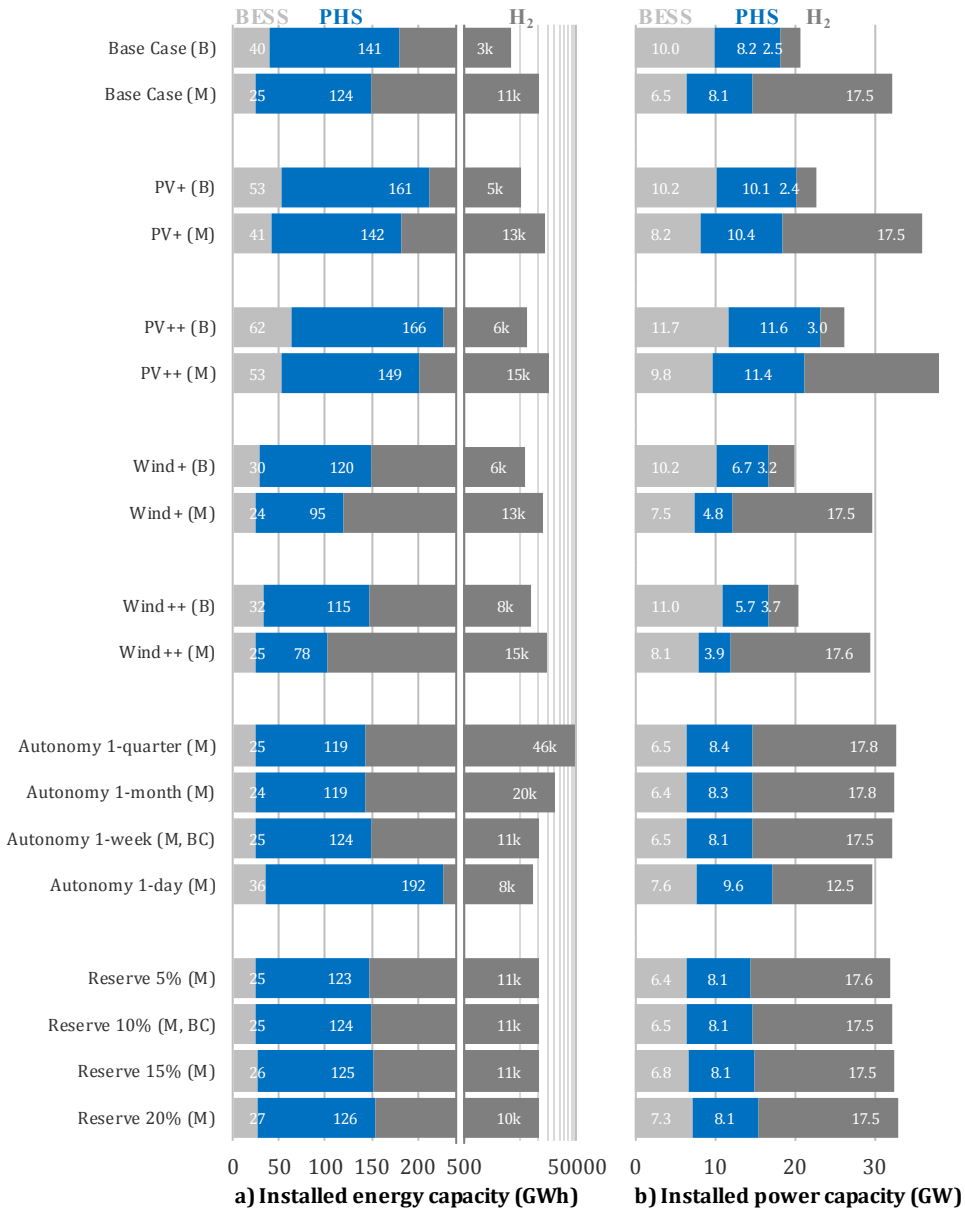

Fig. 4. *Investment decisions of ESS (BESS, PHS, and H_2) in terms of (a) energy capacity and (b) power capacity, for the different scenarios. Note that (a) shows a discontinuous x-axis, which is first linear and then logarithmic.*

Furthermore, when looking at the recommended storage mix, more deviations are found. For BESS, PHS, and H_2, the power capacities in the base case of model B are 10.0, 8.2, and 2.5 GW, respectively, and of model M are 6.5, 8.1, and 17.5 GW. In relative terms, this is a modification by a factor of 0.7, 1.0 and 7.1 for the respective three storage types. This means that H_2 substitutes BESS, while PHS remains invariant. This behavior also holds for the energy capacity. Here, we observe how model B recommends 40, 140, 3220 GWh and model M suggest 25, 124, 10580 GWh for BESS, PHS, and H_2, respectively. Again, in relative terms, this means strong changes between both models: 0.6, 0.9, and 3.3 for the three storage technologies. Perhaps, the increase in energy capacity of H_2 could be expected given its low (energy) investment costs. The substitution of the power capacities (cheap BESS by expensive H_2) is counter-intuitive at first but is related to the multi-services and will be discussed and explained in Section 4.3.3. For the remainder of the discussion, relative numbers will be used.

4.3.2 Sensitivity to PV-to-wind scenarios

The resulting power and energy capacities of ESS for the different renewable scenarios are shown in Table 4 and Table 5. They show how the total power capacity resulting from model M is around 1.4–1.6 times larger than in model B, for all scenarios. The resulting deviations in energy capacity are even larger. These range from 1.9 in wind based scenarios (which do not need as much storage, being consistent with previous studies [10]) and 3.2 in the balance mix scenario. Solar-dominated grids are in between.

Regarding the resulting mix, again, H_2 takes over in all scenarios when including multi-services. Its energy capacity tends to double/triple and its power capacity grows over a factor of five. H_2 displaces the energy capacity of BESS and PHS. In power capacities, H_2 substitutes BESS and PHS up to 30% each. PHS only suffers substantial changes in the wind dominated scenarios.

Table 4: *Power capacity of model M under different PV-to-wind ratios (%, relative to model B)*

Power capacity	BESS	PHS	H_2	Total
Base Case (M)	0.7	1.0	7.1	1.6
PV+ (M)	0.8	1.0	7.2	1.6
PV++ (M)	0.8	1.0	5.8	1.5
Wind+ (M)	0.7	0.7	5.6	1.5
Wind++ (M)	0.7	0.7	4.8	1.4

Table 5: *Energy capacity of model M under different PV-to-wind ratios (%, relative to model B)*

Energy capacity	BESS	PHS	H2	Total
Base Case (M)	0.6	0.9	3.3	3.2
PV+ (M)	0.8	0.9	2.7	2.6
PV++ (M)	0.8	0.9	2.4	2.4
Wind+ (M)	0.8	0.8	2.2	2.2
Wind++ (M)	0.8	0.7	1.9	1.9

4.3.3 Sensitivity to service parameters

In this part, we will analyze how the investment decisions are impacted when considering different parameters for the services. Table 6 shows the resulting differences in power capacity and Table 7 in energy capacity (all changes are here measured relative to the base case of model M, i.e. they are additional to the base case of model M). Recall that energy autonomy is leaving a level of stored energy, and power reserves is leaving a margin in the converters (see section 2.3.3.).

As expected, larger amounts of energy autonomy demand more ESS energy capacity because that service hard-constrains the energy to be stored. How this service impacts the mix is not clear a priori. When requesting more autonomy, H_2 emerges as the most cost-efficient solution (see how its energy capacity in Table 7 grows from 0.8 to 4.3). Once larger H_2 is installed, it can provide other services as well. Consequently, H_2 displaces BESS and PHS. Different parameters of autonomy have essentially no impact on the total power capacity, except when using a small value (1 day) for autonomy. This scenario favors investments in BESS and PHS by about 20% each because they are more cost-efficient on that time scale as opposed to H_2 which is rather long-term.

Variations of power reserve parameters do not show large alterations in the total power and total energy capacities. Furthermore, the resulting mix is only slightly affected. Basically, BESS takes care of stricter operating reserve requirements, without affecting the other technologies. The most stringent power reserve requirement favors the investment of BESS up to 12% and 8% in terms of power and energy capacity, respectively.

Table 6: *Power capacity of model M under different service parameters (%, relative to the base case of model M)*

Power capacity	**BESS**	**PHS**	**H2**	**Total**
Autonomy 1-day	1.2	1.2	0.7	0.9
Autonomy 1-week (BC)	1.0	1.0	1.0	1.0
Autonomy 1-month	1.0	1.0	1.0	1.0
Autonomy 1-quarter	1.0	1.0	1.0	1.0
Reserve 5%	0.98	1.00	1.00	1.00
Reserve 10% (BC)	1.00	1.00	1.00	1.00
Reserve 15%	1.04	1.00	1.00	1.00
Reserve 20%	1.12	1.00	1.00	1.00

Table 7: *Energy capacity of model M under different service parameters (%, relative to the base case of model M)*

Energy capacity	**BESS**	**PHS**	**H2**	**Total**
Autonomy 1-day	1.4	1.5	0.8	0.8
Autonomy 1-week (BC)	1.0	1.0	1.0	1.0
Autonomy 1-month	1.0	1.0	1.9	1.9
Autonomy 1-quarter	1.0	1.0	4.3	4.3
Reserve 5%	0.99	0.99	1.00	1.00
Reserve 10% (BC)	1.00	1.00	1.00	1.00
Reserve 15%	1.03	1.01	1.00	1.00
Reserve 20%	1.08	1.02	0.99	1.00

As a concluding remark of Section 4.3, including energy autonomy and power reserves in expansion planning strongly impacts the investment decisions. Total power capacities and energy capacities turn out to be about 1.4–1.6 and 1.9–3.2 times larger than in traditional planning, for the different scenarios of renewable shares. Using different service parameters creates additional and significant changes in the total energy capacity but more limited ones in total power capacity. The recommended mix is heavily affected under all scenarios, observing a general shift towards hydrogen.

5 Conclusions and future work

In this paper, we developed a novel optimization for planning the expansion of storage and renewable technologies, called LEELO, in which the provision of power reserves and energy autonomy is modeled endogenously. Recall that power reserves and energy autonomy are mechanisms of coping with short-term and long-term forecast errors, respectively. Although these services are relevant for the adequacy of power systems and potentially impact the investment recommendations, they are not usually considered in expansion planning. LEELO is applied to a case study about a 100% renewable grid: the Chilean power system in the year 2050. A whole year with an hourly resolution is modeled, considering three storage (battery, pumped-hydro, and hydrogen) and three generation technologies (wind, solar photovoltaic, and existing hydropower cascades). Different scenarios are evaluated, varying the ratio between wind and solar generation and the service parameters. By implementing two versions of our model, we compared how multi-service planning differs from the conventional energy-based planning.

In terms of operation, ESS show minor differences between both models. All ESS participate in balancing energy fluctuations. As might be expected, batteries (low energy-to-power ratio) provide most of the power reserves (short-term operation), complemented by pumped-hydro during the nights. Hydrogen storage (high energy-to-power ratio) takes care of the energy autonomy (long-term operation). However, the investment recommendations for storage technologies from our multi-services model differ significantly compared to those from conventional planning, attaining power capacities and energy capacities up to 1.6 and 3.2 times larger, respectively. Moreover, the resulting storage mix is profoundly affected. In our multi-service model, batteries are substituted to a large extent by hydrogen storage. Pumped-hydro remains mostly invariant. These findings are consistent for the explored power mixes. Using different parameters for the modeled services changes none of the identified trends, under the considered cost assumptions.

Furthermore, considering power reserves and energy autonomy reveals about 20% higher (total) costs. These costs remain hidden in the traditional energy modeling approach. Therefore the solutions found by traditional planning are suboptimal and cause additional unexpected costs, such as ex-post modifications for upgrades to meet the required levels of service.

Our findings underline the importance of modeling multi-services in the task of planning renewable power systems. Not including these services means in practice obtaining systems that are either unreliable or suffer from large adaptation costs. These results are relevant for all entities that in the aim of meeting the Paris Agreement deal with highly renewable power systems, such as governments, power system planners, regulation entities, and generation companies.

Future work can extend our approach to interactions with other energy sectors (e.g. heat and transport) or by considering other flexibility options in the power sector. We also recommend a more precise definition of the service levels, which is both a technical and political task. Environmental services (life cycle emissions [57] or ecological flows in hydropower operation [50]) could also be evaluated, including the corresponding future pricing mechanisms. Finally, further research on stochastic- or robust-based programming approaches is recommended for additional evaluation of the uncertainty from renewable generation.

Acknowledgments

The authors thank the support of the German Academic Exchange Service (DAAD), the German Research Foundation through the grant DFG-NO 805/11-1, the Chilean Council of Scientific and Technological Research (CONICYT/ FONDAP/15110019, CONICYT/ FONDECYT/1151438), and the Helmholtz Research School on Energy Scenarios.

Appendix

Table 8: *Nomenclature of model: sets, variables, and parameters*

	Name	Units	Description
Sets	$\boldsymbol{t}$		Time steps
	$\boldsymbol{z}$		Zone of the power system
	$\boldsymbol{r}$		Renewable power plants
	$\boldsymbol{s}$		Storage technologies
	$\boldsymbol{h}$		Hydropower plants
Variables (operation)	$p_{t,z,r}$	MW	Power generated by renewable plant r in zone z at time t
	$p_{s,t,z}^{charge}$, $p_{s,t,z}^{discharge}$	MW	Power charged to or discharged from storage s in zone z at time t
	$p_{t,h}$	MW	Power generated by hydropower plant h at time t
	$p_{z,t}^{unserved}$	MW	Power unserved in zone z at time t
	$p_{z,t}^{curtailed}$	MW	Power curtailed in zone z at time t
	$p_{zz,z,t}^{imp}$	MW	Imported power from zone zz to z at time t
	$p_{z,zz,t}^{exp}$	MW	Exported power to zone zz from z at time t
	$oRes_t^{system}$	MW	Operational reserve (total) prescribed by the system at time t
	$oRes_{t,z,s}^{S}$	MW	Operational reserve from storage s in zone z at time t
	$oRes_{t,h}^{H}$	MW	Operational reserve from hydropower in zone z at time t
	$fRes_t^{system}$	MW	Contingency reserve (total) prescribed by the system at time t
	$fRes_{t,z,s}^{S}$	MW	Contingency reserve from storage s in zone z at time t
	$fRes_{t,h}^{H}$	MW	Contingency reserve from hydropower in zone z at time t
	$autonomy_{s,z,t}$	MWh	Autonomy from of storage s in zone z at time t
	$autonomy_{h,t}$	MWh	Autonomy from of hydropower h at time t
	$stored_{s,z,t}$	MWh	Stored energy of storage s in zone z at time t
	$stored_{s,h}$	m^3	Stored water of hydropower h in zone z at time t
	$loss_{s,z,t}^{storage}$	MW	Energy loss (self-discharge) of storage s in zone z at time t
	$loss_{s,z,t}^{reserves}$	MW	Energy loss (provision of reserves) of storage s in zone z at time t
	$loss_{h,t}$	m^3	Water losses (infiltration, evaporation) of hydropower h at time t
	$q_{h,t}^{turbined}$	m^3/s	Flow turbined by hydropower h at time t
	$q_{h,t}^{diverted}$	m^3/s	Flow diverted by hydropower h at time t
	$q_{h,t}^{reserve}$	m^3/s	Flow used for reserve provision by hydropower h at time t
	$q_{h,t}^{fictitious}$	m^3/s	Fictitious flow of hydropower h at time t (used for tuning purposes)
	$q_{h,t}^{turbined\ upstream}$	m^3/s	Flow turbined upstream of hydropower h at time t
	$q_{h,t}^{diverted\ upstream}$	m^3/s	Flow diverted upstream of hydropower h at time t
Variables (investment)	$P_{r,z}^{ins}$	MW	Installed power capacity of renewable technology r in zone z
	P_l^{ins}	MW	Installed power capacity of transmission lines l
	$P_{s,z}^{ins\ dis.}$, $P_{s,z}^{ins\ charge}$	MW	Installed power capacity (discharging, charging) of storage s in zone z
	$E_{s,z}^{ins}$	MWh	Installed energy capacity of storage s in zone z
Inputs	$Load_{t,z}$	MW	Load (demand) in zone z at time t
	P_h^{ins}	MW	Installed power capacity on hydropower h
	$P^{largest\ unit}$	MW	Power capacity of largest (hydro)power generator
	$Profile_{r,t,z}$	%	Profile of renewable source r in zone z at time t
	$P_{max}^{curtailed}$	%	Maximum amount of renewable energy to be curtailed
	$PVtoWindRatio$	%	Proportion between power capacity of PV and wind plants
	η_{charge}, η_{dis}	%	Charging and discharging efficiency of storage s
	$F_s^{Min\ E2P}$, $F_s^{Max\ E2P}$	%	Minimum and maximum energy to power ratio of storage s
	$F^{used\ oRes}$	%	Ratio between the deployed and committed operating power reserves
	$F^{used\ fRes}$	%	Ratio between the deployed and committed frequency power reserves
	$AutomyHours^{system}$	h	Ability of the power system to operate autonomously, in hours
	$Autonomy^{system}$	MWh	Ability of the power system to operate autonomously, in energy
	$E_{s,z}^{potential}$	MWh	Technical potential of energy capacity of storage s in zone z
	k_h	$MW/(m^3/s)$	Yield of hydropower h
	$Q_{h,t}^{inflow}$	m^3/s	Inflow to hydropower h at time t

References

[1] Rogelj J, den Elzen M, Höhne N, Fransen T, Fekete H, Winkler H, et al. Paris Agreement climate proposals need a boost to keep warming well below 2 °C. Nature 2016;534:631–9. doi:10.1038/nature18307.

[2] Pamparana G, Kracht W, Haas J, Díaz-Ferrán G, Palma-Behnke R, Román R. Integrating photovoltaic solar energy and a battery energy storage system to operate a semi-autogenous grinding mill. J Clean Prod 2017;165:273–80. doi:10.1016/j.jclepro.2017.07.110.

[3] Rahmann C, Vittal V, Ascui J, Haas J. Mitigation Control Against Partial Shading Effects in Large-Scale PV Power Plants. IEEE Trans Sustain Energy 2016;7:173–80. doi:10.1109/TSTE.2015.2484261.

[4] Steinke F, Wolfrum P, Hoffmann C. Grid vs. storage in a 100% renewable Europe. Renew Energy 2013;50:826–32. doi:10.1016/j.renene.2012.07.044.

[5] Clegg S, Mancarella P. Integrated Electrical and Gas Network Flexibility Assessment in Low-Carbon Multi-Energy Systems. IEEE Trans Sustain Energy 2016;7:718–31. doi:10.1109/TSTE.2015.2497329.

[6] U. S. Department of Energy. Global Energy Storage Database 2018. http://www.energystorageexchange.org/projects (accessed September 1, 2018).

[7] Child M, Breyer C, Bogdanov D, Fell H-J. The role of storage technologies for the transition to a 100% renewable energy system in Ukraine. Energy Procedia 2017;135:410–23. doi:10.1016/j.egypro.2017.09.513.

[8] Barthelemy H, Weber M, Barbier F. Hydrogen storage: Recent improvements and industrial perspectives. Int J Hydrogen Energy 2017;42:7254–62. doi:10.1016/j.ijhydene.2016.03.178.

[9] Budt M, Wolf D, Span R, Yan J. A review on compressed air energy storage: Basic principles, past milestones and recent developments. Appl Energy 2016;170:250–68. doi:10.1016/j.apenergy.2016.02.108.

[10] Cebulla F, Haas J, Eichman J, Nowak W, Mancarella P. How much electrical energy storage do we need? A synthesis for the U.S., Europe, and Germany. J Clean Prod 2018;181:449–59. doi:10.1016/j.jclepro.2018.01.144.

[11] Cebulla F, Naegler T, Pohl M. Electrical energy storage in highly renewable European energy systems: Capacity requirements, spatial distribution, and storage dispatch. J Energy Storage 2017;14:211–23. doi:10.1016/j.est.2017.10.004.

[12] Bussar C, Stöcker P, Cai Z, Moraes L, Magnor D, Wiernes P, et al. Large-scale integration of renewable energies and impact on storage demand in a European renewable power system of 2050-Sensitivity study. J Energy Storage 2016;6:1–10. doi:10.1016/j.est.2016.02.004.

[13] Kilickaplan A, Bogdanov D, Peker O, Caldera U, Aghahosseini A, Breyer C. An energy transition pathway for Turkey to achieve 100% renewable energy powered electricity, desalination and non-energetic industrial gas demand sectors by 2050. Sol Energy 2017;158:218–35. doi:10.1016/j.solener.2017.09.030.

[14] Gulagi A, Bogdanov D, Fasihi M, Breyer C. Can Australia Power the Energy-Hungry Asia with Renewable Energy? Sustainability 2017;9:233. doi:10.3390/su9020233.

[15] Haas J, Cebulla F, Cao K-K, Nowak W, Palma-Behnke R, Rahmann C, et al. Challenges and trends of energy storage expansion planning for flexibility provision in low-carbon power systems – a review. Renew Sustain Energy Rev 2017;80:603–19. doi:10.1016/j.rser.2017.05.201.

[16] Labadie JW. Optimal Operation of Multireservoir Systems: State-of-the-Art Review. J Water Resour Plan Manag 2004;130:93–111. doi:10.1061/(ASCE)0733-9496(2004)130:2(93).

[17] Ortiz JMH, Pourakbari-Kasmaei M, López J, Mantovani JRS. A stochastic mixed-integer conic programming model for distribution system expansion planning considering wind generation. Energy Syst 2018;9:551–71. doi:10.1007/s12667-018-0282-z.

[18] Santos SF, Fitiwi DZ, Bizuayehu AW, Shafie-khah M, Asensio M, Contreras J, et al. Novel Multi-Stage Stochastic DG Investment Planning with Recourse. IEEE Trans Sustain Energy 2017;8:164–78. doi:10.1109/TSTE.2016.2590460.

[19] Asensio M, Meneses de Quevedo P, Munoz-Delgado G, Contreras J. Joint Distribution Network and Renewable Energy Expansion Planning Considering Demand Response and Energy Storage—Part I: Stochastic Programming Model. IEEE Trans Smart Grid 2018;9:655–66. doi:10.1109/TSG.2016.2560339.

[20] Dominguez ODM, Kasmaei MP, Mantovani JRS. Adaptive Robust Short-Term Planning of Electrical Distribution Systems Considering Siting and Sizing of Renewable Energy-based DG Units. IEEE Trans Sustain Energy 2018.

[21] Haas J, Cebulla F, Nowak W, Rahmann C, Palma-Benhke R. A multi-service approach for planning the optimal mix of energy storage technologies in a fully renewable power supply. Under Rev 2018.

[22] Pudjianto D, Aunedi M, Djapic P, Strbac G. Whole-Systems Assessment of the Value of Energy Storage in Low-Carbon Electricity Systems. IEEE Trans Smart Grid 2014;5:1098–109. doi:10.1109/TSG.2013.2282039.

[23] Schill W-P, Zerrahn A. Long-run power storage requirements for high shares of renewables: Results and sensitivities. Renew Sustain Energy Rev 2018;83:156–71. doi:10.1016/J.RSER.2017.05.205.

[24] Ministerio de Energía. Energía 2050 - Proceso participativo politica energetica (Participatory process for the Energy Policy 2050). Santiago: 2015.

[25] Jimenez-Estevez G, Palma-Behnke R, Roman Latorre R, Moran L. Heat and Dust: The Solar Energy Challenge in Chile. IEEE Power Energy Mag 2015;13:71–7. doi:10.1109/MPE.2014.2380012.

[26] Saboori H, Hemmati R, Abbasi V. Multistage distribution network expansion planning considering the emerging energy

storage systems. Energy Convers Manag 2015;105:938–45. doi:10.1016/j.enconman.2015.08.055.
[27] Shabanpour-Haghighi A, Seifi AR. Simultaneous integrated optimal energy flow of electricity, gas, and heat. Energy Convers Manag 2015;101:579–91. doi:10.1016/j.enconman.2015.06.002.
[28] GAMS Software GmbH. GAMS 2017.
[29] IBM. IBM ILOG CPLEX Optimization Studio 2018.
[30] Haller M, Ludig S, Bauer N. Decarbonization scenarios for the EU and MENA power system: Considering spatial distribution and short term dynamics of renewable generation. Energy Policy 2012;47:282–90. doi:10.1016/j.enpol.2012.04.069.
[31] Novosel T, Ćosić B, Pukšec T, Krajačić G, Duić N, Mathiesen BV, et al. Integration of renewables and reverse osmosis desalination – Case study for the Jordanian energy system with a high share of wind and photovoltaics. Energy 2015;92:270–8. doi:10.1016/j.energy.2015.06.057.
[32] Rajesh K, Karthikeyan K, Kannan S, Thangaraj C. Generation expansion planning based on solar plants with storage. Renew Sustain Energy Rev 2016;57:953–64. doi:10.1016/j.rser.2015.12.126.
[33] Cebulla F, Fichter T. Merit order or unit-commitment: How does thermal power plant modeling affect storage demand in energy system models? Renew Energy 2017;105:117–32. doi:10.1016/J.RENENE.2016.12.043.
[34] Zerrahn A, Schill WP. Long-run power storage requirements for high shares of renewables: review and a new model. vol. 79. Pergamon; 2017. doi:10.1016/j.rser.2016.11.098.
[35] Erdölbevorratungsverband. Erdölbevorratungsverband 2018.
[36] Belderbos A, Virag A, D'haeseleer W, Delarue E. Considerations on the need for electricity storage requirements: Power versus energy. Energy Convers Manag 2017;143:137–49. doi:10.1016/j.enconman.2017.03.074.
[37] Kühne M. Drivers of energy storage demand in the German power system : an analysis of the influence of methodology and parameters on modelling results. Technische Universität München, 2016.
[38] Haas J. Inputs for LEELO (Long-term Energy Expansion Linear Optimization) (Version v38/v39) [Data set] 2018. doi:10.5281/zenodo.1344412.
[39] Breyer C, Afanasyeva S, Brakemeier D, Engelhard M, Giuliano S, Puppe M, et al. Assessment of mid-term growth assumptions and learning rates for comparative studies of CSP and hybrid PV-battery power plants. AIP Conf Proc 2017;1850. doi:10.1063/1.4984535.
[40] Kousksou T, Bruel P, Jamil A, El Rhafiki T, Zeraouli Y. Energy storage: Applications and challenges. Sol Energy Mater Sol Cells 2013;120:59–80. doi:10.1016/j.solmat.2013.08.015.
[41] Coordinador Eléctrico Nacional (Chile's Power System Operator). Public information system 2017. https://www.coordinadorelectrico.cl/sistema-informacion-publica/.
[42] Bogdanov D, Koskinen O, Aghahosseini A, Breyer C. Integrated renewable energy based power system for Europe, Eurasia and MENA regions. 2016 Int Energy Sustain Conf IESC 2016 2016. doi:10.1109/IESC.2016.7569508.
[43] Alvarez R, Moser A, Rahmann CA. Novel Methodology for Selecting Representative Operating Points for the TNEP. IEEE Trans Power Syst 2017;32:2234–42. doi:10.1109/TPWRS.2016.2609538.
[44] National Energy Commission of Chile (CNE). Informe Preliminar de Previsión de Demanda 2016-2036, SIC-SING (Report on the demand projection for 2016-2036 in Central and Northern Chile). Santiago, Chile: 2016.
[45] Valhalla. Espejo de Tarapacá Project 2017. http://valhalla.cl/espejo-de-tarapaca/ (accessed September 4, 2017).
[46] Schaeffer C, Smits M. From matters of fact to places of concern? Energy, environmental movements and place-making in Chile and Thailand. Geoforum 2015;65:146–57. doi:10.1016/j.geoforum.2015.07.021.
[47] Inzunza A, Moreno R, Bernales A, Rudnick H. CVaR constrained planning of renewable generation with consideration of system inertial response, reserve services and demand participation. Energy Econ 2016;59:104–17. doi:10.1016/j.eneco.2016.07.020.
[48] Coordinador Eléctrico Nacional (Chile's Power System Operator). Inflows to hydropower plants n.d. https://sic.coordinador.cl/en/informes-y-documentos/fichas/estadistica-de-caudales-afluentes/ (accessed January 31, 2018).
[49] Haas J, Olivares MA, Palma-Behnke R. Grid-wide subdaily hydrologic alteration under massive wind power penetration in Chile. J Environ Manage 2015;154:183–9. doi:10.1016/j.jenvman.2015.02.017.
[50] Olivares MA, Haas J, Palma-Behnke R, Benavides C. A framework to identify Pareto-efficient subdaily environmental flow constraints on hydropower reservoirs using a grid-wide power dispatch model. Water Resour Res 2015;51:3664–80. doi:10.1002/2014WR016215.
[51] Department of Geophysics - University of Chile, Ministry of Energy of Chile. Explorador de energía solar (Solar energy explorer) 2012. http://walker.dgf.uchile.cl/Explorador/Solar2/ (accessed August 25, 2015).
[52] Department of Geophysics - University of Chile, Ministry of Energy of Chile. Explorador de energía eólica (Wind power explorer) 2012. http://ernc.dgf.uchile.cl/Explorador/Eolico2/ (accessed August 21, 2013).
[53] Molina A, Falvey M, Rondanelli R. A solar radiation database for Chile. Sci Rep 2017;7:1–11. doi:10.1038/s41598-017-13761-x.
[54] Haas J, Palma-Behnke R, Valencia F, Araya P, Díaz-Ferrán G, Telsnig T, et al. Sunset or sunrise? Understanding the barriers and options for the massive deployment of solar technologies in Chile. Energy Policy 2018;112:399–414. doi:10.1016/j.enpol.2017.10.001.

[55] Kamalinia S, Shahidehpour M, Khodaei A. Security-constrained expansion planning of fast-response units for wind integration. Electr Power Syst Res 2011;81:107–16. doi:10.1016/j.epsr.2010.07.017.

[56] Hemmati R, Hooshmand R-A, Khodabakhshian A. Comprehensive review of generation and transmission expansion planning. IET Gener Transm Distrib 2013;7:955–64. doi:10.1049/iet-gtd.2013.0031.

[57] Moreno-Leiva S, Díaz-Ferrán G, Haas J, Telsnig T, Díaz-Alvarado F a., Palma-Behnke R, et al. Towards solar power supply for copper production in Chile: Assessment of global warming potential using a life-cycle approach. J Clean Prod 2017;164:242–9. doi:10.1016/j.jclepro.2017.06.038.